Computers and Electronics in Agriculture 90 (2013) 63–67

Contents lists available at SciVerse ScienceDirect

Computers and Electronics in Agriculture

journal homepage: www.elsevier.com/locate/compag

# Development of a structure analysis algorithm on structures from $CuCl_2{\cdot}2H_2O$ crystallization with agricultural products ☆

Paul Doesburg [a,*], Andreas F.M. Nierop [b]

[a] Louis Bolk Institute, Driebergen, The Netherlands
[b] Muvara BV, Leiderdorp, The Netherlands

ARTICLE INFO

*Article history:*
Received 8 June 2012
Received in revised form 12 October 2012
Accepted 7 November 2012

*Keywords:*
Crystallization
Dihydrate Copper chloride
Texture analysis
Structure analysis
Physiological processes
Food quality

ABSTRACT

Crystallization patterns emerge when an aqueous dihydrate Copper chloride ($CuCl_2{\cdot}2H_2O$) solution in the presence of organic additives (juices/extracts) is crystallized on a glass plate. The emerging patterns are additive-specific and reflect physiological processes like maturation and ageing, the effect of processing, feeding regime and production system in a broad range of agricultural products. The patterns and their underlying structures are evaluated visually by means of defined morphological criteria and by means of computerized image analysis, respectively. The currently applied texture analysis algorithm reflects the spatial linear relationships between grey-scale values of the scanned crystallization structures, rendering the zero point arbitrary and constraining data analysis to the ordinal scale. Furthermore the algorithm is non-consistent with the physically defined geometric properties of the crystallization structures.

In this article the development of a structure analysis algorithm is described and discussed which allows a quantification of the crystallization structures by computing 15 width-, and length-parameters, introducing a non-arbitrary zero-point and an equidistant scale which permits all statistical measures. The algorithm is applied to crystallization structures produced from carrot samples which shows it reflects the monotonic relation between physically defined geometric properties of the crystallization structures and laboratory procedure parameters influencing the overall morphological features of the crystallization structures. For instance the nucleation time, which is the time elapsed prior to initial nucleation of the crystallization structure, and the circular region of interest (ROI) around the geometric center of the glass plate used in image analysis evaluation. It is concluded that this structure analysis algorithm is a valuable addition to the image evaluation tools applicable for crystallization investigations of agricultural products, augmenting the image analysis with a non-arbitrary zero point and an equidistant scale which permits all statistical measures.



## 1. Introduction

Crystallization patterns emerge when an aqueous dihydrate Copper chloride ($CuCl_2{\cdot}2H_2O$) solution is crystallized on a glass plate in the presence of organic additives (Busscher et al., 2010a). The emerging patterns are additive-specific (Andersen et al., 2001), and reflect physiological processes like maturation and ageing, the effect of processing, feeding regime and production system in a broad range of agricultural products (Weibel et al., 2001; Kahl et al., 2009; Szulc et al., 2010; Fritz et al., 2011). Hence the interest in the method from an organistic quality perspective (Bloksma et al., 2007; Kahl et al., 2012).

The crystallization patterns and their underlying structures are evaluated visually on the basis of defined morphological criteria (Huber et al., 2010), and by means of computerized texture analysis (Andersen et al., 1999; Meelursarn, 2007), respectively. The computerized evaluation of the crystallization structures enables a standardization of the method, which revealed the main source of variation to be the crystallization process itself (Busscher et al., 2010b). Consequently studies elucidating the physical conditions underlying the crystallization process are ongoing (Busscher et al., 2010a).

The crystallization structures exhibit a dendritic nature resulting in a hierarchical order of first-, second-, and higher-level branches. The currently used texture grey level co-occurrence matrix (GLCM) algorithm reflects the spatial linear relationships between grey-scale values thus making it less suited for the analysis of structures. The output is non-consistent with the physically defined geometric properties of the crystallization structures, which is demonstrated by an inability to reflect the monotonic

*Abbreviations:* ROI, region of interest; GLCM, grey level co-occurrence matrix.

☆ The work described in this article has been carried out in accordance with the uniform requirements for manuscripts submitted to biomedical journals.

* Corresponding author. Present address: Crystal Lab – Focus on Food Quality, Kleefseweg 9, NL-6595NK Ottersum, The Netherlands. Tel.: +31 (0)485 769009.
*E-mail address:* p.doesburg@crystal-lab.nl (P. Doesburg).

0168-1699/$ - see front matter © 2012 Elsevier B.V. All rights reserved.
http://dx.doi.org/10.1016/j.compag.2012.11.003

relation between physically defined geometric properties of the crystallization structures and procedure parameters influencing the overall morphological features. For instance the procedure parameter nucleation time which is the time elapsed prior to initial nucleation of the crystallization structure (Busscher et al., 2010b), and the procedure parameter circular region of interest (ROI) around the geometric center of the glass plate used in image analysis evaluation. Moreover, this non-consistency with physically defined geometric properties of the crystallization structures renders the zero point in the texture analysis output arbitrary, constraining data analysis to the ordinal scale (Kahl et al., 2010).

In this article the development and application of a structure analysis algorithm is discussed which allows a quantification of physically defined morphological properties of the crystallization structures by quantifying 15 width-, and length-parameters, thereby introducing a non-arbitrary zero point and an equidistant scale which permits all statistical measures (Stevens, 1946).

## 2. Materials and methods

Copper(II) chloride dihydrate pro analysis was purchased from Merck (Ref. #1.02733.1000) and dissolved in milli-Q water (Millipore) at a final concentration of 0.59 mol $l^{-1}$.

Carrot samples (Daucus carota L.) originated from a field trial (Hessische Staatsdomäne Frankenhausen, Germany) of the University of Kassel from harvest 2004 (Fleck et al., 2005). For the present study, bulk samples of the two cultivated varieties Rodelika and Rothild at nitrate fertilizer levels 0 and 150 kg N $ha^{-1}$ were crystallized according to standard laboratory procedures for carrots (Busscher et al., 2010b). Samples were prepared in three-fold repetition in one chamber on three consecutive days, resulting in 27 plates per sample and 108 plates in total. Per plate, 115 mg sieved juice (calculated as 115 μl sieved juice) and 90 mg $CuCl_2$ was used.

The nucleation time was monitored with a camera mounted on the ceiling of the chamber (Busscher et al., 2010a). To evaluate to which extent the texture-, and structure analysis algorithms reflect the monotonic relation between different physically defined geometric properties of the crystallization structures and the procedure parameter nucleation time, 25 crystallization plates originating from Rodelika 0 kg N $ha^{-1}$, from one experimental day were divided into five groups exhibiting an increasing nucleation time. Group one having a nucleation time from 11:30 to 12:11 (hours after pipetting the solution into the dish), group two from 12:11 to 12:51, group three from 12:56 to 13:50, group four from 14:16 to 14:56 and group five from 14:56 to 15:50.

Crystallization plates were converted to RGB images by transmission scanning using a PowerLook III UMAX Scanner (Busscher et al., 2010b). A total of 15 second-order variables at resolution scale one were computed for ROIs 20-90% at 10% intervals. The statistical evaluation was carried out by means of a 'linear-mixed-effects' model with repeated measurements via crossed effects, programmed in R (version 2.1.0) (Meelursarn, 2007). The results of this statistical evaluation ($F$ and $p$-values) were plotted relative to the ROIs. Only variables showing a monotonous course over the ROI were considered for evaluation.

### 2.1. Computing the binary crystallization structure

The structure analysis algorithm is developed with Matlab[1] (version 7.7.0 R2008b, Mathworks Inc., Natick, Massachusetts). The scanned RGB image files were converted to the corresponding grey-scale images with the Matlab function rgb2grey, which converts RGB images to grey-scale based on the luminance information by forming a weighted sum of the R, G, and B components (30%R, 59%G, 11%B). Image segmentation to binaries is performed by threshold selection with local mean grey-scales $A$, calculated on the basis of a four pixel-diameter disk, and threshold scalar $b$, which is computed as $0.8^*$ the mean of $A$ within the default 90% ROI. Prior to image segmentation, the local mean grey-scales $A$ were adapted with $A_{new} = 0.8^*(A_{old} - b) + b$ which decreases the significance of local noise compared to thresholding based on local averages alone. A series of Matlab bwmorph morphological operations was performed to optimize the resulting binary by successively filling isolated interior pixels (0's surrounded by 1's) and deleting isolated pixels (1's surrounded by 0's) not belonging to the overall crystallization structure. Cross-points were added for local ' + ' shaped connections having a missing central pixel. During the entire process of smoothing, image segmentation and morphological transformation detailed enlarged visual comparisons were made by overlaying the original scanned RGB image and the binary derivative to verify structural conservation in all its detail, simultaneously securing for the introduction of spurious structural elements that could interfere with subsequent analysis.

### 2.2. Characterization of the binary crystallization structure

The binary crystallization structure can be characterized on the basis of width and length parameters. To determine the widths of the binary, each pixel's distance to the local outer boundary in the binary crystallization structure was calculated with the Matlab function bwdist using the image complement. This assigns a number corresponding to the Euclidean distance between that pixel and the nearest non-zero pixel. The local maxima of these distances, representing the middle of the branches, were multiplied with two to represent the local widths and subsequently binned into 15 logarithmically equally spaced containers: D20 representing a maximum diameter of 2 pixels, D24 representing a diameter between 2 and 2.4 pixels, likewise for D29, D35, D41, D48, D55, D64, D73, D83, D94, D107, D120, and D134, and ending with D150 representing all diameters greater than 13.4 pixels. For image presentation each local maximum is replaced by a colored droplet representing the respective container, thereby depicting the crystallization structures as paintings, painted with colored drops in a Van Gogh like style. Thus 15 colored brushes are used to make the droplet representations. The process of painting the images is started with small droplets upon which gradually larger brushes are selected (see Figs. A.1 and B.1). The quantification of the 15 colored widths is performed by measuring the surface covered at different ROIs enabling a characterization of the binary crystallization structure. The surface not covered by the 15 widths is labeled as D0. Likewise the crystal-free surfaces, i.e., the areas where no Copper chloride deposits are found, can be characterized by applying the procedure described above on the complement of the binary crystallization structure.

Crystallization branches emanate from nodes, consequently a distinction is made in the structure analysis algorithm between internodal and terminal branches. The ends of the terminal branches are defined as end-points. The frequency of branching, and therefore the length of the internodal and terminal branches, is a second relevant morphological criterion aiding the characterization of the crystallization structures.

The nodes, end-points and the internodal and terminal branches were characterized by skeletizing the binary crystallization structure with the Matlab function bwmorph, applying the morphological operation 'thin'. Local square $3 \times 3$ filtering was subsequently used to detect the end-points and the nodes. Mini

[1] A general accessible documentation of the used Matlab functions is available online at http://www.mathworks.nl/help/pdf_doc/images/images_tb.pdf (version R2012a).

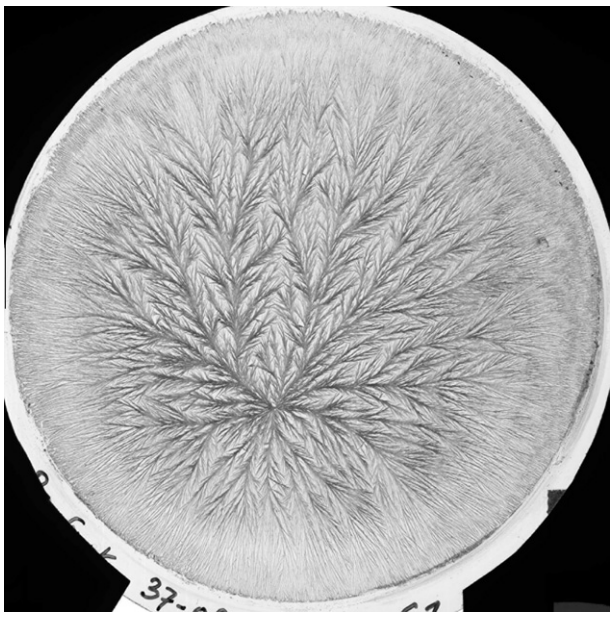

**Fig. A.1.** Original scanned RGB image, carrot variety Rodelika 0 kg N ha$^{-1}$.

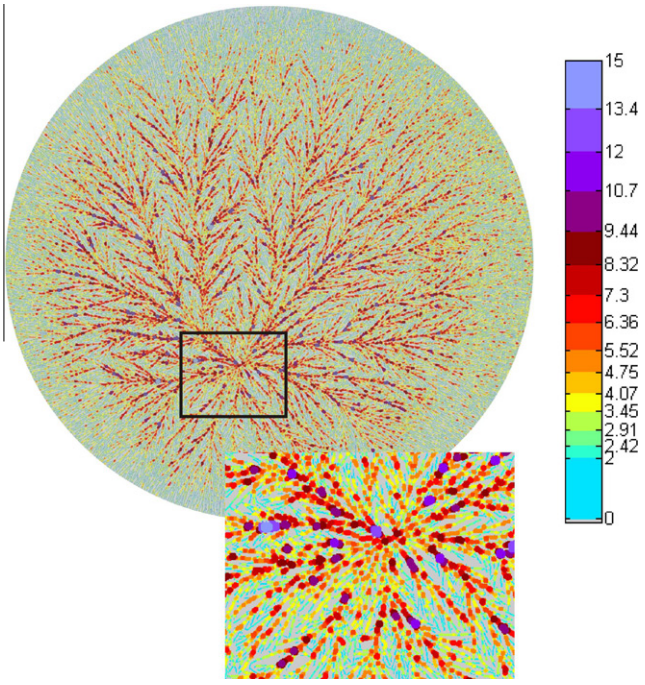


**Fig. B.1.** Top left: painted droplet representation of the scanned crystallization structure in Fig. A.1, characterized on the basis of the 15 width parameters (top right). Below: enlarged image visualizing the individual painted droplets representing the different width parameters.

networks of intertwined branches were split into nodes and very short branches by defining locally filtered valid and non-valid one pixel internodal connections. In addition, branches which exceeded a predefined curvature were split too. For this, the maximum deviation from a hypothetical straight line between the two extremes comprising the branch was computed. A split was forced when the maximum deviation exceeded 1.5 pixels and the split-point's distance from either extreme was larger than three pixels. The lengths of all branches were binned into 15 logarithmically equally spaced containers: L20 representing a maximum length of 2 pixels, L26 representing a length between 2 and 2.6 pixels, likewise for L33, L41, L51, L62, L75, L89, L108, L124, L144, L167, L192, L220, and ending with L250 representing all lengths exceeding 22 pixels. For image presentation each of the 15 lengths were replaced by a colored line of one-pixel width representing the respective container. Furthermore nodes (Lnode), split-points (Lsplit) and end-points (Lend) are colored as single pixels respectively in grey, white and black. The resulting sketch resembles a hand-made (line) drawing. The quantification of the 15 lengths, the nodes, the split-points and the end-points is performed by measuring the surface covered at different ROIs enabling a second characterization of the binary crystallization structure. The surface not covered by the 15 lengths, nodes, split-, and end-points is labeled L0. Likewise the crystal-free surfaces can be characterized too by applying the procedure described above on the complement of the binary crystallization structure.

## 3. Results

### 3.1. Texture analysis

The 15 second-order texture analysis variables can be divided into three groups of positively correlated variables (Meelursarn, 2007). These three groups are represented by the variables Diagonal moment, Kappa and Sum variance (Carstensen, 1992), results will be discussed accordingly.

The differentiation between the two carrot varieties was significant for all three group-variables ($p < 0.001$, ROI < 90%) (Busscher et al., 2010b). The largest differentiation was observed between the two carrot strains at 0 kg N ha$^{-1}$ by the variable Sum variance with $F = 110$ at ROI 70%. There was no differentiation found between the two nitrate fertilizer levels for either carrot variety.

To visualize the extent to which the different variables reflect the monotonic dependency between physically defined geometric properties of the crystallization structure and the two procedure parameters, the three group-variables were plotted relative to the ROIs 20–90%. As illustrated for Kappa in Fig. C.1, the relation with the nucleation time is only monotonic at specific ROIs (90% for both Kappa and Sum variance), whereas the relation is non-monotonic for Diagonal moment over the entire ROI-range. In a similar way the second procedure parameter, evaluated ROI, was assessed. In Fig. D.1 the relation between the evaluated ROI and Sum variance is non-monotonic. Similar results were found for the other two group-variables.

### 3.2. Structure analysis

The differentiation between the two carrot varieties was significant for multiple variables ($p < 0.001$, ROI > 20%). The largest differentiation was observed between the two carrot strains at 0 kg N ha$^{-1}$ by the variable D0 with $F = 180$ at ROI 50%. A significant differentiation was found between the two nitrate fertilizer levels for variety Rothild only, with L250 ($p < 0.001$, ROI > 70%, $F = 33$ at ROI 80%), and to a lesser extent with the variables L106 ($p < 0.001$, ROI 80–90%) and L89, L124, Lsplit ($p < 0.001$, ROI 90%).

To visualize the extent to which the different variables reflect the monotonic dependency between physically defined geometric properties of the crystallization structure and the two procedure parameters, all variables were plotted relative to the ROIs 20–90%. As illustrated for L250 in Fig. E.1, the relation between the nucleation time and L250 is monotonic over the whole ROI-range. Similar results were found for all other variables. In a similar way the second procedure parameter, evaluated ROI, was assessed. In Fig. F.1, the relation between the evaluated ROI and D120 is monotonic over the whole ROI-range. Similar results were found for all other variables.

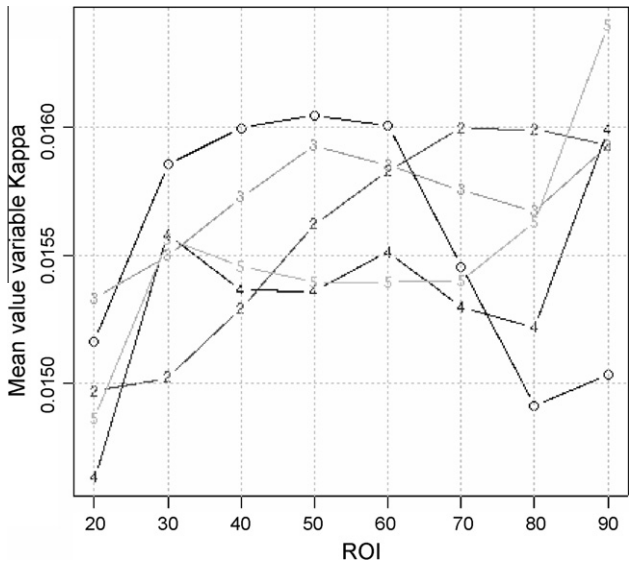


**Fig. C.1.** Mean value texture analysis variable Kappa plotted against the analyzed ROI for crystallizations produced from carrot variety Rodelika 0 kg N ha$^{-1}$. Group 0 having a nucleation time from 11:30 to 12:11 (hours after pipetting), group 2 from 12:11 to 12:51, group 3 from 12:56 to 13:50, group 4 from 14:16 to 14:56 and group 5 from 14:56 to 15:50.

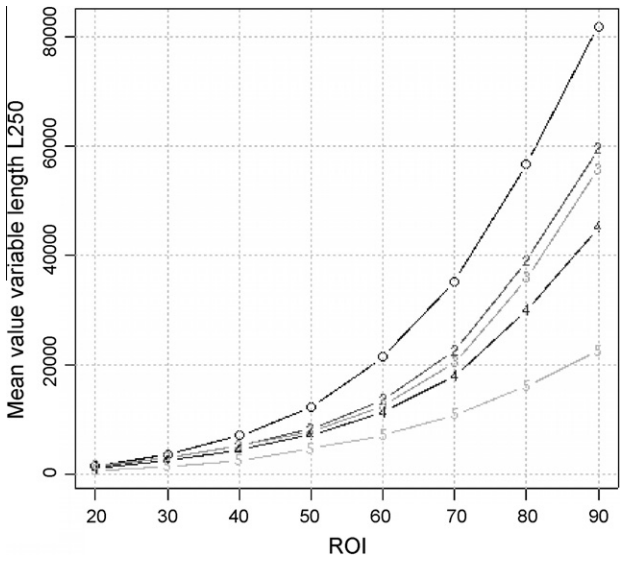


**Fig. E.1.** Mean value structure analysis variable L250 plotted against the analyzed ROI for crystallizations produced from carrot variety Rodelika, 0 kg N ha$^{-1}$. Group 0 having a nucleation time from 11:30 to 12:11 (hours after pipetting), group 2 from 12:11 to 12:51, group 3 from 12:56 to 13:50, group 4 from 14:16 to 14:56 and group 5 from 14:56 to 15:50.

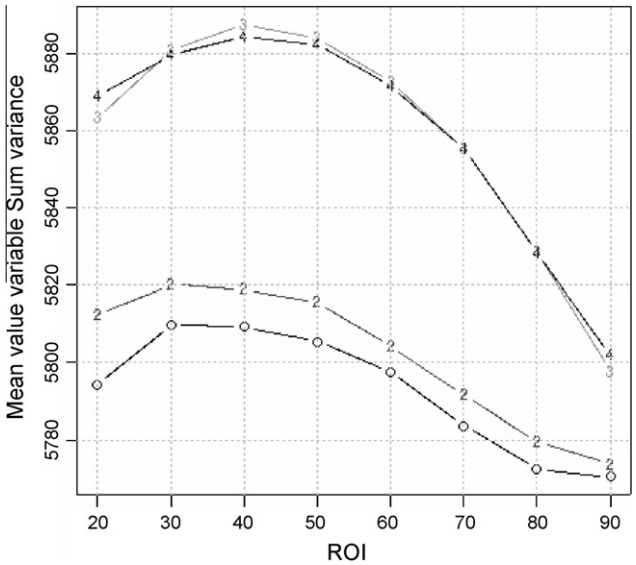


**Fig. D.1.** Mean value texture analysis variable Sum variance plotted against the analyzed ROI. Group 0 for crystallizations produced from Rodelika, 0 kg N ha$^{-1}$, group 2 for Rodelika, 150 kg N ha$^{-1}$, group 3 for Rothild, 0 kg N ha$^{-1}$ and group 4 for Rothild, 150 kg N ha$^{-1}$.

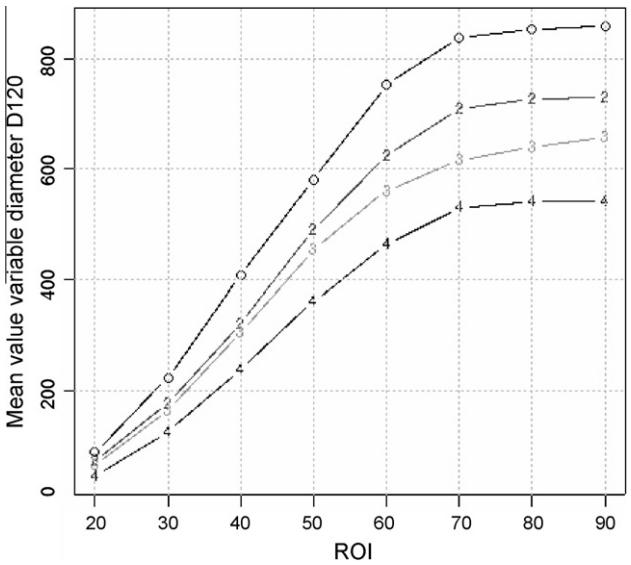


**Fig. F.1.** Mean value structure analysis variable D120 plotted against the analyzed ROI. Group 0 for crystallizations produced from Rodelika, 0 kg N ha$^{-1}$, group 2 for Rodelika, 150 kg N ha$^{-1}$, group 3 for Rothild, 0 kg N ha$^{-1}$ and group 4 for Rothild, 150 kg N ha$^{-1}$.

## 4. Discussion

Visual evaluation of patterns from $CuCl_2{\cdot}2H_2O$ crystallization with additives shows there is a reproducible variation of morphological criteria of the image in relation to the nucleation time (Busscher et al., 2010b). The currently used texture analysis GLCM algorithm reflects the spatial linear relationships between grey-scale values of the scanned crystallization structures and consequently is generally imperceptive for this dependency. Furthermore, the algorithm is non-consistent with the physically defined geometric properties of the crystallization structures. For the novel structure analysis algorithm, allowing a quantification of 15 width-, and length parameters, including the nodes, split-points and end-points, this dependency is apparent. The algorithm reflects the monotonic dependency between physically defined geometric properties of the crystallization structure and the procedure parameters nucleation time and evaluated ROI (Figs. E.1 and F.1).

The two here discussed algorithms reflect two conceptually different approaches to image segmentation (i.e., the partitioning of an image into its different areas of interest). To estimate the positioning of these approaches relative to one another within the field of image segmentation a categorization is used based on a conceptualization of the currently available image segmentation methodologies[2] (Dey et al., 2010). This categorization is following a coarse-

[2] Recommendation for further reading: Richards, J.A., 2012. Remote sensing digital image analysis, an introduction. 5th ed. Springer-Verlag, Germany.

to-fine sequence. The categories are highly interrelated, consequently image segmentation methodologies generally combine approaches from all three categories. The first category comprises model driven (top-down) and image driven (bottom-up) approaches, which can either be supervised or unsupervised. The second category comprises homogeneity based approaches which are subdivided into increasing degrees of complexity based on the considered features: primary (spectral/textural), secondary (shape and size), tertiary (context) and quaternary (temporal). The third category comprises operations to segment an object from an image (e.g., edge detection, region growing/splitting). The two applied algorithms in this article can thus be characterized as unsupervised, image driven, homogeneity based approaches of the primary (texture analysis algorithm) and the secondary (structure analysis algorithm) level.

In the light of the above it is concluded that the structure analysis algorithm provides a valuable addition to the image evaluation tools applicable for crystallization investigations of agricultural products, augmenting the image analysis with a non-arbitrary zero point and an equidistant scale which permit all statistical measures.

## Role of the funding sources

The funding foundations had no role in study design, in the collection, analysis and interpretation of data, in the writing of the report and in the decision to submit the paper for publication.

## Acknowledgements

The authors thank the Software AG-Stiftung and the Phoenix foundation for their financial support for this work. Dr. J. Kahl is thanked for discussions and feedback.

## References

Andersen, J.-O., Henriksen, C., Laursen, J., Nielsen, A., 1999. Computerised image analysis of biocrystallograms originating from agricultural products. Comput. Electron. Agric. 22, 51–69.

Andersen, J.-O., Kaack, K., Nielsen, M., Thorup-Kristensen, Kr., Labouriau, R., 2001. Comparative study between biocrystallization and chemical analysis of carrots (Daucus carota L.) grown organically using different levels of green manures. BAH 19, 29–48.

Bloksma, J., Northolt, M., Huber, M., van der Burgt, G.J., van de Vijver, L.P.L., 2007. A new food quality concept based on life processes. In: Cooper, J., Niggli, U., Leifert, C. (Eds.), Handbook of Organic Food Safety and Quality. Woodhead Publishing, Cambridge, UK, pp. 53–73.

Busscher, N., Kahl, J., Doesburg, P., Mergardt, G., Ploeger, A., 2010a. Evaporation influences on the crystallization of an aqueous dihydrate cupric chloride solution with additives. J. Colloid Interface Sci. 334, 556–562.

Busscher, N., Kahl, J., Andersen, J.-O., Huber, M., Mergardt, G., Doesburg, P., Paulsen, M., Ploeger, A., 2010b. Standardization of the biocrystallization method for carrot samples. BAH 27, 1–23.

Carstensen, J. M., 1992. Description and simulation of visual texture. Ph.D thesis, Technical University of Denmark, Lyngby, Denmark.

Dey, V., Zhang, Y., Zhong, M., 2010. A review on image segmentation techniques with remote sensing perspective. In: Wagner W., Székely, B. (Eds.), ISPRS TC VII Symposium – 100 Years ISPRS, Vienna, Austria, vol. XXXVIII, July 5–7, 2010, IAPRS, Part 7A.

Fritz, J., Athmann, M., Kautz, T., Köpke, U., 2011. Grouping and classification of wheat from organic and conventional production systems by combining three image forming methods. BAH 27, 320–336.

Fleck, M., von Fragstein, P., Heß, J., 2005. Ertrag und Zuckergehalte bei Möhren nach Applikation der biologisch-dynamischen Präparate Hornmist und Hornkiesel in verschiedenen Umwelten. Tagungsband 8. Wissenschaftstagung Ökolandbau, Kassel, pp. 89–93.

Huber, M., Andersen, J.-O., Kahl, J., Busscher, N., Doesburg, P., Mergardt, G., Kretschmer, S., Zalecka, A., Meelursarn, A., Ploeger, A., Nierop, D., van de Vijver, L., Baars, E., 2010. Validation of the visual evaluation of biocrystallizations. development of a reliable and valid instrument for visual evaluation according to ISO-Norms for sensory analyses. BAH 27, 25–40.

Kahl, J., Busscher, N., Doesburg, P., Mergardt, G., Huber, M., Ploeger, A., 2009. First tests of standardized biocrystallization on milk and milk products. Eur. Food Res. Technol. 229, 175–178.

Kahl, J., Busscher, N., Ploeger, A., 2010. Questions to the validation of holistic methods testing organic food quality. BAH 27, 81–94.

Kahl, J., Baars, T., Bügel, S., Busscher, N., Huber, M., Kusche, D., Rembialkowska, E., Schmid, O., Seidel, K., Taupier-Letage, B., Velimirov, A., Zalecka, A., 2012. Organic food quality: a framework for concept, definition and evaluation from the European perspective. J. Sci. Food Agric. http://dx.doi.org/10.1002/jsfa.5640.

Meelursarn, A., 2007. Statistical evaluation of texture analysis from the biocrystallization method: Effect of image parameters to differentiate samples from different farming systems. PhD thesis, University of Kassel. Witzenhausen, Germany.

Stevens, S., 1946. On the theory of scales of measurement. Science 103, 677–680.

Szulc, M., Kahl, J., Busscher, N., Mergardt, G., Doesburg, P., Ploeger, A., 2010. Discrimination between organically and conventionally grown winter wheat farm pair samples using the copper chloride crystallization method in combination with computerised image analysis. Comput. Electron. Agric. 74, 218–222.

Weibel, F., Bickel, R., Leuthold, S., Alföldi, T., Niggli, U., Balzer-Graf, U., 2001. Bioäpfel – besser und gesünder? Eine Vergleichsstudie mit Standard und Alternativmethoden der Qualitätserfassung. Ökologie und Landbau 177, 25–28.